HIGHLY ORGANIZED
CATALYTIC SYSTEMS

Nanocomposites Based on LaCoO₃ and Mesoporous Molecular Sieves: Preparation and Physicochemical and Catalytic Properties

E. V. Makshina*, S. V. Sirotin*, V. V. Yushchenko*, G. N. Mazo*, M. W. E. van den Berg**, K. V. Klement'ev**, W. Grünert**, and B. V. Romanovskii*

* Department of Chemistry, Moscow State University, Moscow, 117234 Russia
** Laboratory of Industrial Chemistry, Ruhr University, Bochum, Germany
Received October 12, 2004

Abstract—Individual perovskite-like $LaCoO_3$ obtained by the citrate method and $LaCoO_3$ supported onto the mesoporous molecular sieve MSM-41 have been characterized by X-ray powder diffraction, EPMA, low-temperature nitrogen adsorption, H_2 TPR, and EXAFS. The catalytic activity of the supported cobaltate in methanol oxidation is two orders of magnitude higher than the activity of the bulk cobaltate owing to nanosized $LaCoO_3$ particles in the pores of the molecular sieve.

Conventional catalysts for the oxidation of organic substances are Group VIII metals supported on an oxide matrix with a developed surface. Although these catalysts have obvious advantages, their application is limited not only by the high cost of the noble metals but also by the considerable volatility of the noble metal oxides and by their high sinterability. Alternative catalytic systems are perovskite-like mixed oxides of composition ABO_3, where A is a lanthanide cation and B is a transition metal cation. In some cases, the oxidation efficiency of perovskites approaches or even exceeds the oxidation efficiency of Pt-containing catalysts [1, 2]. This property of the perovskites is primarily due to the fact that their structure has an almost unique capacity for stabilizing various transition metals in atypical oxidation states. Furthermore, the perovskites as catalysts can be modified by replacing part of their A atoms with heterovalent atoms and thereby changing the proportions of B atoms in different oxidation states. Lastly, a fundamentally important factor in oxidative catalysis is the high mobility of the structural oxygen of the perovskites, which allows oxygen atoms to participate directly in the elementary oxidation event and brings about oxygen vacancies, which serve as O_2 chemisorption sites [2–6].

At the same time, perovskites, which are usually obtained by the high-temperature sintering of a mixture of oxide precursors, have a specific surface area no larger than a few tens of square meters per gram [1, 2]. This drawback makes them less attractive as catalytic systems. There have been multiple attempts to increase their specific surface area by *in situ* high-temperature synthesis on the surface of inorganic supports such as mesoporous silica gel and alumina [7, 8] impregnated with appropriate metal salts. However, the materials thus obtained appeared to be catalytically ineffective because of the formation, on their surface, of silicates or aluminates, which are inactive in oxidation, instead of perovskites [8]. Furthermore, the broad pore-radius distribution inherent in these and similar supports prevents the formation of monodisperse particles of the supported active component. This negates all the advantages of the *in situ* synthesis.

The above difficulties in the preparation of finely dispersed supported perovskites can be circumvented in a number of ways. The first way is to use a mixed citrate, oxalate, or cyanide complex as the precursor instead of a mixture of salts. Such a complex can be converted to a perovskite at a much lower temperature [9]. The second way is to support the catalyst onto a mesoporous molecular sieve, such as MSM-41, with a specific surface area of the order 1000 m²/g and with a mesoporous structure formed by nonintersecting channels of uniform size (3–10 nm). For the first time, this synthetic route was used by Nguyen *et al.* [10], who obtained composites consisting of the molecular sieve MSM-41 and the mixed oxide $LaCoO_3$ (10–50 wt %) incorporated in its pores. However, Nguyen *et al.* [10] presented only indirect evidence that a perovskite, not a mixture of oxides, was formed inside the channels.

Here, we report a comparative study of the physicochemical and catalytic properties of unsupported $LaCoO_3$ that was obtained from a citrate complex and had a typical perovskite structure, supported $LaCoO_3$ obtained from the same complex by *in situ* synthesis in the mesopores of MSM-41, and a mechanical mixture of La_2O_3 and Co_3O_4 with equal atomic fractions of lanthanum and cobalt. This study has provided insights

into the nature of the nanoparticles forming in the support pores.

EXPERIMENTAL

Synthesis of the Citrate Complex

The citrate complex of La and Co was obtained by a known procedure [11]. Equimolar amounts of lanthanum and cobalt nitrates (La, 0.005 mol; Co, 0.005 mol) were dissolved in 100 ml of an aqueous solution of citric acid (0.010 mol). The molar ratio of citric acid to La + Co was 1 : 1. The solution (citrate precursor) was continuously stirred at room temperature for 24 h and was then used in the synthesis of unsupported and supported lanthanum cobaltate. Furthermore, we prepared cobalt citrate in order to synthesize cobalt oxide.

Synthesis of the Unsupported Perovskite

For the synthesis of the unsupported perovskite and unsupported cobalt oxide, the solution of the citrate complex or cobalt citrate (prepared as described above) was evaporated for several hours at 100°C to obtain a dry residue. This residue was calcined in air at 600°C for 8 h.

For comparison, we prepared, by thorough mixing, a mechanical mixture of lanthanum and cobalt oxides with La : Co = 1 : 1.

Synthesis of the Supported Perovskite

Supported lanthanum cobaltate was obtained by impregnating a support with a solution of the lanthanum–cobalt citrate complex. Air-dry mesoporous MSM-41[1] (2.2 g) was impregnated with the solution (20 ml) of the citrate precursor to obtain a catalyst containing ~10 wt % supported perovskite. The product was dried at 60–65°C and then calcined at 600°C for 8 h in flowing air. The supported cobaltate thus obtained is hereafter designated $LaCoO_3$/MSM-41.

Physicochemical Methods

Specific surface areas were measured by the nitrogen BET method using an ASAP 2000 instrument.

Phase analysis was carried out by X-ray diffraction on a DRON-3M diffractometer (filtered CuK_α radiation; $2\theta = 20°–80°$).

Temperature-programmed reduction (TPR) with hydrogen was carried out as follows. A sample (50 mg) was placed into a quartz reactor, and the reactor was heated to 400°C at a rate of 6 K/min in flowing dry argon (30 ml/min) and was held at this temperature for 1 h. Thereafter, it was cooled to room temperature and switched to an argon–hydrogen mixture containing

---

[1] The authors are grateful to E.E. Knyazeva for help with the synthesis of the molecular sieve MSM-41.

3.5 vol % H_2. Next, the temperature was raised at a constant rate of 7 K/min, and the reduction rate of the sample was derived from hydrogen uptake data between 20 and 1000 K. The total amount of hydrogen consumed in the reduction process was derived from the area under the H_2 TPR curve.

The cationic composition of surfaces was determined by EPMA using a JEOL JSM-840A scanning electron microscope fitted with a PGT IMIX system.

EXAFS transmission spectra near the cobalt absorption *K*-edge were obtained on an E4 spectrometer (Laboratory of Synchrotron Radiation, DESY Research Center, Hamburg) using an Si(111) double-crystal monochromator. The spectra were recorded at room temperature in the energy range 7500–8800 eV.

Study of Catalytic Properties

Methanol conversion was studied in a flow catalytic microreactor between 150 and 200°C. A catalyst sample (250–300 mg) was placed into the reactor and was held at 200°C in flowing air for 2 h. Thereafter, the preset temperature was established and the reactor was switched to a methanol–air mixture fed at a rate of 60 ml/min, which corresponds to a methanol molar feed rate of $v = 5.6$ mmol/h. The composition of the reaction product was determined by GLC. Oxygen-containing compounds (methanol, dimethyl ether, and formaldehyde) were quantified on an M-3700 chromatograph using a flame-ionization detector, a 3-m-long column packed with Carbowax-20M and thermostated at 50°C, and nitrogen as the carrier gas. CO_2 was determined on a CHROM-5 chromatograph in a temperature-programmed mode, using a thermal-conductivity detector and a 5-m-long column packed with Porapak Q. Chromatograms were recorded and processed using an Ekokhrom hardware–software complex.

The total methanol conversion was no higher than 15%. For this reason, the rate of the partial and complete oxidations of methanol was determined as $w = vx_i/(100m)$, where x_i is the conversion of methanol to formaldehyde or CO_2 and m is the weight of the active component of the sample charged into the reactor.

RESULTS AND DISCUSSION

The properties of the materials synthesized are presented in the table.

According to X-ray diffraction data, unsupported $LaCoO_3$ has a perovskite structure and contains no lanthanum oxide or cobalt oxide phase. Cobalt oxide obtained by the decomposition of cobalt citrate is single-phase and has a spinel structure. By contrast, the supported material $LaCoO_3$/MSM-41 is amorphous to X-rays: its diffraction pattern shows no reflections assignable to a perovskite structure or any other oxide phase. On the one hand, this result possibly indicates

Chemical and phase composition and texture properties of the materials examined

Material	Phase composition	Chemical composition, wt %		Atomic ratio	
		La	Co	La	Co
LaCoO$_3$	Perovskite	50.1	22.0	1	1
LaCoO$_3$/MCM-41	Supported cobaltate	5.53	2.46	1	1
La$_2$O$_3$ + Co$_3$O$_4$	Mechanical mixture of oxides	56.9*	24.1*	1	1

* Calculated percentage of metal in the mechanical mixture.

that the oxidative thermal decomposition of the citrate complex in the channels of MSM-41 yields nanoparticles. Indeed, the pore diameter in MSM-41 is about 3 nm, which is much below the size of a coherent-scattering region. On the other hand, a disordered product phase would likewise give no reflections.

Atomic-resolution EPMA data obtained from six different points of the LaCoO$_3$/MSM-41 surface indicate the formation of a chemically homogeneous product phase. Within the measurement error, the La : Co atomic ratio is nearly the same for all of these points and is consistent with the stoichiometry of lanthanum cobaltate. Since a casual coincidence is unlikely in these series of measurements, it is believed that the LaCoO$_3$ phase rather than a mixture of oxides forms in the MSM-41 pores.

According to low-temperature nitrogen adsorption data, the specific surface area of unsupported perovskite is 10.4 m^2/g and that of unsupported cobalt oxide is 7.4 m^2/g. These results are in good agreement with an earlier report on cobaltates obtained by the citrate method [2]. The specific surface area of LaCoO$_3$/MSM-41 is 680 m^2/g, which differs only slightly from the value of 690 m^2/g determined for the original support. The outer surface area of the molecular sieve is relatively small. Therefore, if any considerable part of the total amount of supported cobaltate

(10 wt %) were formed on this surface, the inlets of all of the support pores would be blocked. The absence of reflections from oxide phases, which could occupy any area on the surface, suggests that only little, if any, cobaltate is located on the outer surface of the molecular sieve. Thus, in the thermal decomposition of citrate precursors in the pores of the mesoporous support MSM-41, almost all of the resulting cobaltate resides inside the pores.

Supported lanthanum cobaltate and unsupported perovskite were also studied by EXAFS spectroscopy. An analysis of the near fine structure of the XANES spectrum has demonstrated that the average oxidation state of cobalt in the supported cobaltate is +2, while the oxidation state of cobalt in the unsupported perovskite is +3. At the same time, the shape of the absorption peak indicates the absence of Co$_3$O$_4$ particles in LaCoO$_3$/MSM-41 (Fig. 1).

An analysis of the extended fine structure (EXAFS region; Fig. 2) revealed obvious distinctions between the state of cobalt in supported and bulk LaCoO$_3$. The spectrum of bulk LaCoO$_3$ shows well-defined photon scattering signals from several coordination spheres. In the supported cobaltates, there is no ordered structure beyond the first coordination sphere of cobalt. The diffuse signal between 2 and 3 Å is assignable to photon scattering on Co, La, and Si in the second coordination
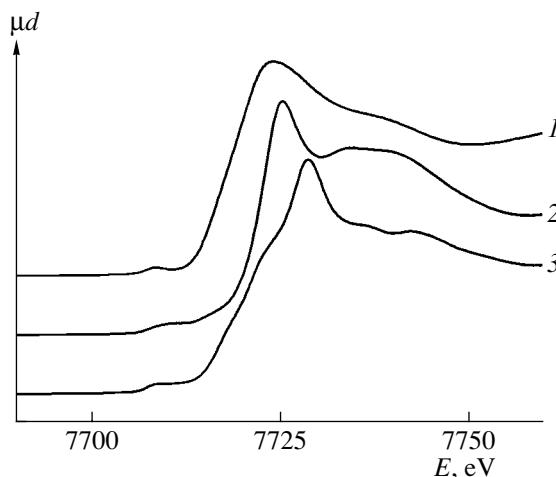

Fig. 1. XANES spectra of (*1*) LaCoO$_3$/MSM-41, (*2*) LaCoO$_3$, and (*3*) Co$_3$O$_4$.
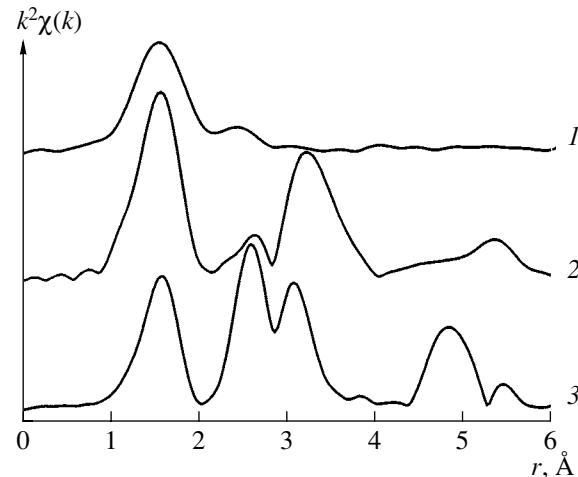

Fig. 2. EXAFS spectra of (*1*) LaCoO$_3$/MSM-41, (*2*) LaCoO$_3$, and (*3*) Co$_3$O$_4$.
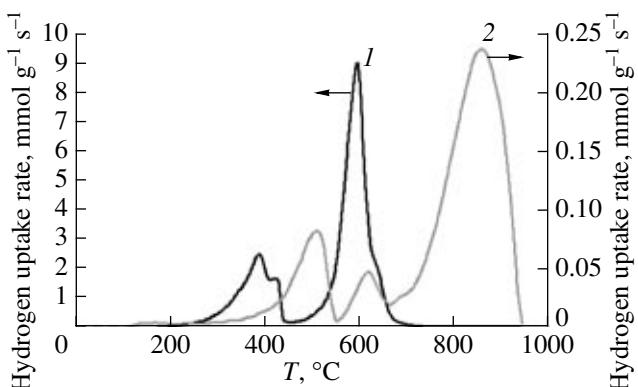
Fig. 3. Hydrogen TPR curves for (*1*) LaCoO$_3$ and (*2*) LaCoO$_3$/MSM-41.

Fig. 4. Rate of methanol conversion to formaldehyde and CO$_2$ (*w*) on (*1*) La$_2$O$_3$ + Co$_3$O$_4$, (*2*) LaCoO$_3$, and (*3*) LaCoO$_3$/MSM-41 at 100, 150, and 200°C.

sphere. This kind of spectrum may be due to a very small particle size and, accordingly, a considerable structural disorder in the supported cobaltate particles, which manifests itself as X-ray amorphism. This inference is confirmed by XANES data: it is likely that a mixed cobaltate containing both Co^{3+} and Co^{2+} cations is present in the supported samples.

The H$_2$ TPR curves for the materials synthesized are presented in Fig. 3. These curves show a number of well-defined hydrogen uptake peaks due to cobalt reduction. The unsupported perovskite is characterized by two reduction peaks [12]. The first, which occurs at 390°C, is due to the one-electron reduction of Co^{3+}. The corresponding hydrogen uptake is precisely equal to the amount of hydrogen required for the formation of a compound of composition LaCoO$_{2.5}$. The higher temperature peak, which is observed at 590°C, arises from the three-electron reduction of Co^{3+} to Co^0. The total amount of hydrogen required for the complete reduction of LaCoO$_3$ to lanthanum oxide and cobalt metal is nearly equal to the stoichiometric amount. For the supported sample, the reduction peaks are markedly shifted to higher temperatures. This shift may arise from the very small size of the particles resulting from the decomposition of the citrate complex in the channels of the matrix [13, 14]. Another argument in favor of this interpretation of the shift of the H$_2$ TPR peaks of LaCoO$_3$/MSM-41 is that the observed hydrogen uptake (0.9 mol H$_2$/mol Co) is much lower than is required for the stoichiometric reaction (1.5 mol H$_2$/mol Co for the complete reduction of Co^{3+} to cobalt metal). Indeed, as was demonstrated by Baiker *et al.* [15], the reduction of cobalt in pure perovskites is complete below 700°C and is accompanied by the formation of a lanthanum oxide phase detectable by X-ray diffraction. By contrast, according to our H$_2$ TPR data, the reduction of the ultrafine perovskite particles in LaCoO$_3$/MSM-41 is incomplete even at 1000°C.

However, there is another plausible explanation for the nonstoichiometric consumption of hydrogen in the reduction of cobalt in the supported perovskite. The marked difference between the observed and calculated H$_2$ uptakes may be due to an extraordinarily high concentration of oxygen vacancies induced in the ultrafine perovskite particles. Estimating the oxygen stoichiometry of these particles leads to the composition LaCoO$_{2.4}$. This composition of the cobaltate implies the presence of cobalt in the oxidation state +2. Indeed, the presence of Co^{2+} is confirmed by EXAFS data.
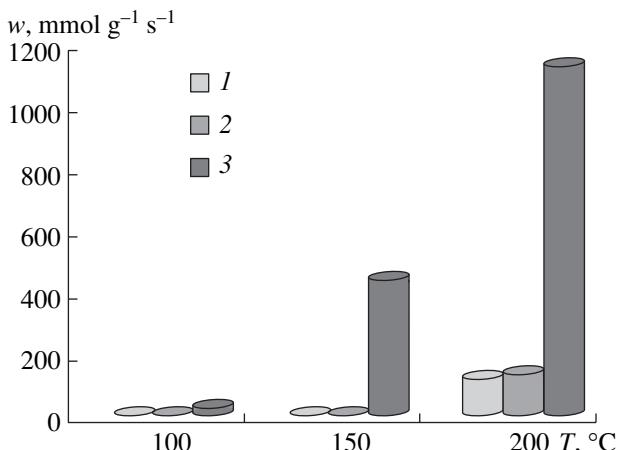
Thus, our physicochemical measurements indicate the formation of LaCoO$_{3-\delta}$ nanoparticles rich in oxygen vacancies in the pores of the mesoporous support MSM-41. This finding is in agreement with the data characterizing the catalytic activity of the bulk and supported perovskite specimens synthesized.

The results of our catalytic tests are presented in Fig. 4. Note that, for all of the catalysts examined, the only methanol conversion reaction is oxidation. None of the catalysts causes methanol dehydration to dimethyl ether.

The unsubstituted cobaltate LaCoO$_3$ supported on MSM-41 shows an extraordinarily high activity as compared to the unsupported perovskite and a mechanical mixture of lanthanum and cobalt oxides. This is apparently due to the presence of a considerable amount of Co^{2+} in the catalyst. Alternatively, the strong activating effect of the mesoporous molecular sieve on lanthanum cobaltate can be explained by the much larger number of oxygen vacancies in the LaCoO$_3$ formed in the nanopores. Indeed, on the assumption that the surfaces of the unsupported and supported perovskites contain equal concentrations of oxygen vacancies as catalytic sites, the difference between the methanol oxidation rates on these catalysts, which is as large as two orders of magnitude, can arise only from an increase in specific surface area from 10 to 1000 m^2/g. The latter value is physically implausible, since it implies that supported perovskite particles are as small as ~0.3 nm. Therefore, the increase in catalytic activity

on passing from the pure perovskite to the perovskite supported on the mesoporous molecular sieve MSM-41 is due to the appearance of Co^{2+} and, at the same time, an increase in the concentration of oxygen vacancies.

Thus, the above physicochemical and catalytic-activity data for the lanthanum cobaltate–based systems examined demonstrate that the citrate method for supporting mixed oxides onto mesoporous materials affords intrapore nanoparticles that are much more active in methanol oxidation than bulk perovskites.

REFERENCES

1. Arai, H., Yamada, T., Eguchi, K., *et al.*, *Appl. Catal.*, 1986, vol. 26, p. 265.
2. Tejuca, L.G., Fierro, J.L.G., and Tascon, J.M.D., *Adv. Catal.*, 1989, vol. 36, p. 237.
3. Wachowski, L. and Laniecki, M., *Acta Chim. Hung.*, 1987, vol. 124, p. 449.
4. Chan, K.S., Ma, J., Jaenicke, S., *et al.*, *Appl. Catal., A*, 1994, vol. 107, p. 201.
5. Tascon, J.M.D., Fierro, J.L.G., and Tejuca, L.G., *Z. Phys. Chem.*, 1981, vol. 124, p. 249.
6. Viswanathan, B. and George, S., *Indian J. Technol.*, 1985, vol. 23, p. 470.
7. Mizuno, N., Fujii, H., and Misono, M., *Chem. Lett.*, 1986, p. 1333.
8. Mizuno, N., *Catal. Today*, 1990, vol. 8, p. 221.
9. Tascon, J.M.D., Mendioroz, S., and Tejuca, L.G., *Z. Phys. Chem.*, 1981, vol. 124, p. 109.
10. Nguyen, S.V., Szabo, V., Trong On, D., *et al.*, *Microporous Mesoporous Mater.*, 2000, vol. 54, p. 5.
11. Baythoun, M.S.G. and Sale, F.R., *J. Mater. Sci.*, 1982, vol. 17, p. 2757.
12. Futai, M., Yonghua, C., and Hui, L., *React. Kinet. Catal. Lett.*, 1986, vol. 31, p. 47.
13. Chernavskii, P.A., *Doctoral (Chem.) Dissertation*, Moscow: Moscow State Univ., 2001.
14. Joyner, R. and Stockenhuber, M., *J. Phys. Chem. B*, 1999, vol. 103, p. 5963.
15. Baiker, A., Marti, P.E., Keusch, P., *et al.*, *J. Catal.*, 1994, vol. 146, p. 268.